OSIRIS

Optical, Spectroscopic, and Infrared Remote Imaging System

In-field stray-light determination and correction

RO-RIS-MPAE-TN-093
Issue: 1
Revision: d
10 May 2022

Prepared by:
Gabor Kovacs

Approval Sheet

2 Aug. 2022

prepared by: Gabor Kovacs (signature/date)

2/8.22

approved by: Holger Sierks (signature/date)

Document Change Record

Iss./Rev.	Date	Author	Pages affected	Description
D / -	14 Mar 2019	Kovacs	all	first draft
D / a	28 May 2019	Kovacs/ Tubiana	all	Revised version
1 / -	3 Jun 2019	Kovacs/ Tubiana	all	First issue
1 / a	17 Oct 2019	Tubiana	Sect. 5 all	Updated criteria for generation of GS images Corrected spelling of stray-light/stray light
1 / b	13 Jul 2020	Güttler	Sect. 5, 7	Clarify condition for SY generation Explicitly list NAC filters with no ghost kernel and remove from database listing
1 / c	20 Dec 2021	Deller	All	Added the following files to the data: 'NAC_FM_GHOST_31_V01.TXT' 'NAC_FM_GHOST_81_V01.TXT' Expanded description of algorithm that used a fixed binning of 4x4
1 / d	10 May 2022	Güttler	Sect. 5	Updated description under which conditions synthetic images are generated

Table of contents

List of Figures

List of Tables

1 General aspects

1.1 Scope

This document describes the method and results of the OSIRIS Narrow Angle Camera (NAC) and Wide Angle Camera (WAC) in-field stray-light analysis. The analysis was carried out using in-flight science and calibration data and using on-ground calibration images acquired using the OSIRIS ground reference model (GRM). The resulting data is used by the OSIRIS calibration pipeline (OsiCalliope, see RD2) to generate in-field stray-light corrected images.

1.1 Reference Documents

no.	document name	document number, Iss./Rev.
RD1	OSIRIS user manual	RO-RIS-MPAE-MA-004, D/s
RD2	OSIRIS calibration pipeline OsiCalliope	RO-RIS-MPAE-MA-007
RD3	Rosetta-OSIRIS To Planetary Science Archive Interface Control Document	RO-RIS-MPAE-ID-015
RD4	Kovacs et al. (2013): Stray light calibration of the Dawn Framing Camera, in SPIE Conf. Ser., 8889, 12	
RD5	Keller et al. (2007): OSIRIS The Scientific Camera System Onboard Rosetta, Space Science Reviews, 128, 433.	

1.2 Acronyms and Abbreviations

ARP	Anti Reflection Plate
CG	Comet 67P/Churyumov-Gerasimenko
DN	Digital numbers, i.e., counts on the CCD
FM	Flight Model
GRM	Ground Reference Model
NAC	Narrow Angle Camera
OSIRIS	Optical, Spectroscopic, and Infrared Remote Imaging System
WAC	Wide Angle Camera

2 In-field stray light and integrated ghost of the camera system

The in-field stray light is an additional signal caused by multiple reflections of the incoming image-forming light within the optical system. For NAC in the orange/red region a ghost intensity of less than 10^{-3} was required [RD1, RD5]. To achieve low in-field stray light, anti-reflective coatings were applied on the optical component surfaces and on the CCD.

The primary sources of in-field stray light are the components near the image plane of the cameras: the CDD detector, the anti-radiation plate (ARP), the band-pass filters and the focusing plates (Figure 1). There are two types of reflection: reflections internal to the optical component (i.e. between the two surfaces of the ARP) and reflection between the surfaces of different components (i.e. between the CCD and the ARP).

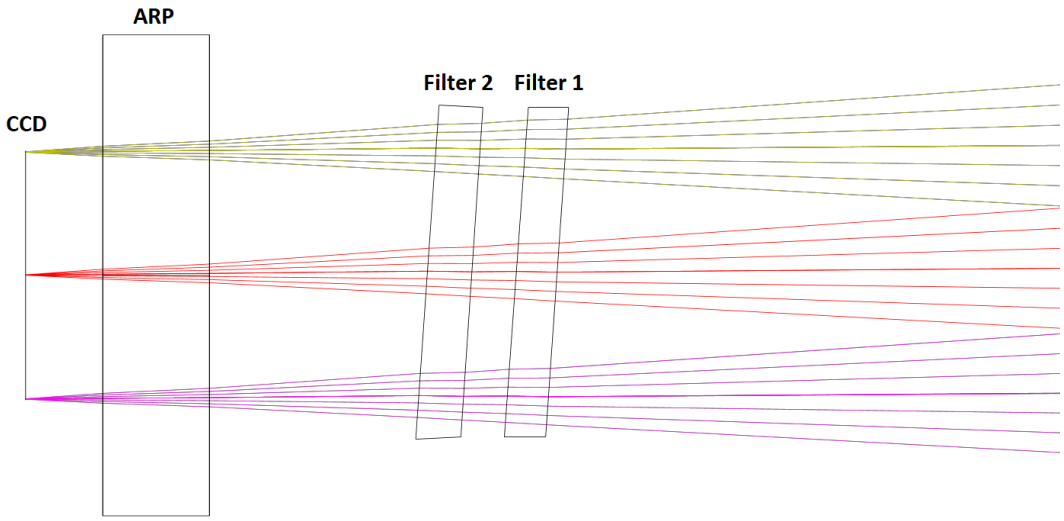

Figure 1 NAC optical components near the image plane. From left to right: The CCD located at the image plane, the thick silica Anti-Radiation Plate (ARP) and two filters.

The optical components create multiple reflections, resulting in ghosts with different size, position, and intensity (Figure 2):

- The highest intensity but usually smallest size ghost component is generated by internal reflections of the image forming rays inside the ARP and the filter surfaces (Figure 2, left).
- The CCD is the source of the Narcissus ghost, by generating multiple reflections between itself and the plane optical surfaces of the ARP and the filters (Figure 2, center).
- Several reflection paths between the different ARP and filter surfaces also add to the ghost contribution, with a smaller intensity, but larger pattern sizes (Figure 2, right).

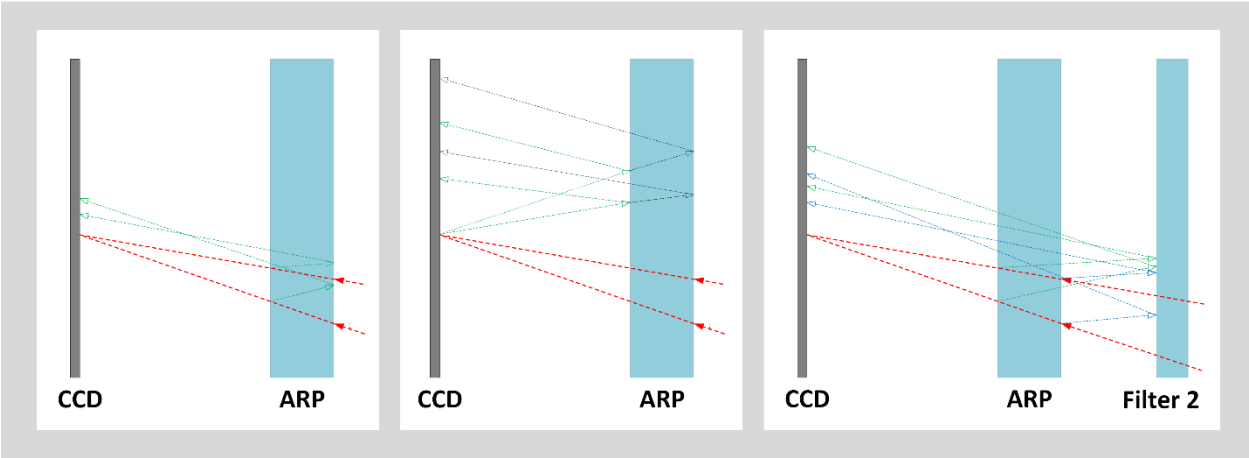

Figure 2 Stray-light paths in the optical system. The image forming rays are marked red. Left: Internal reflections in the ARP. Center: Narcissus ghost reflections between the CCD and the ARP surfaces. Right: Reflections between different optical components (ARP and Filter 2).

The in-field stray-light pattern on the CCD is very complex, with the multiple ghost components overlapping (Figure 3). The correction algorithm targets the strongest 7 components for the NAC and 8 for the WAC, which are responsible for the majority of the in-field stray light.

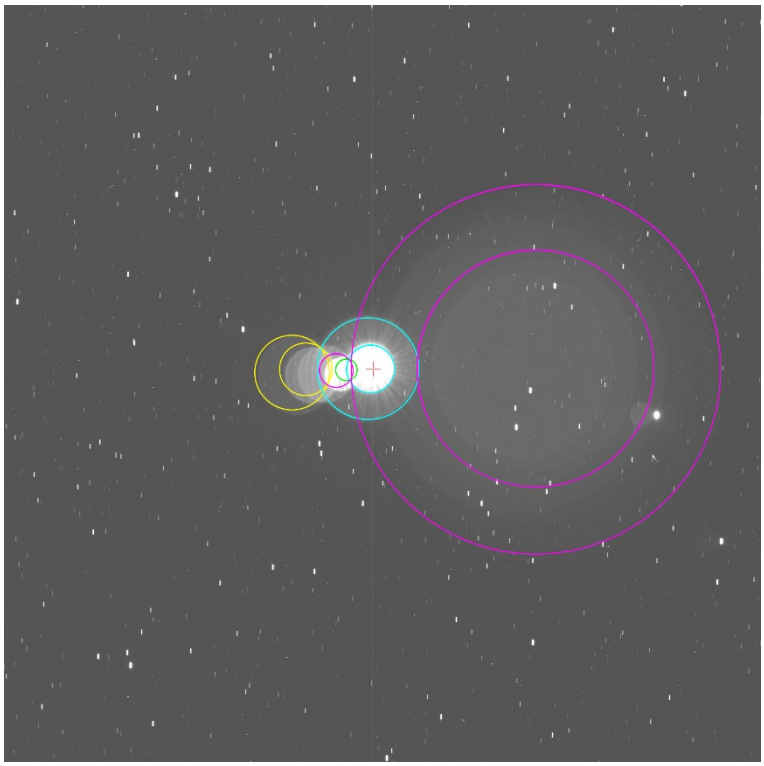

Figure 3 Example of in-field stray-light patter for the NAC F21. Colored contours are overlaid to the image to better visualize the individual ghosts produced by the different optical components.

The in-field stray-light patterns of the NAC and WAC are different, because of the optical layout of the cameras (2 mirror off-axis system of the WAC and 3 mirror for the NAC). The ghost pattern of the WAC is simpler, since only one filter is in the optical path. In addition, because of the highly off-axis optical layout of the WAC, the ghost pattern appears only on one side of the illuminated area (Figure 4, right). The NAC has a smaller principal ray angle, which results in the in-field stray-light pattern appearing on both sides (and around) of the illuminated area (Figure 4, left).

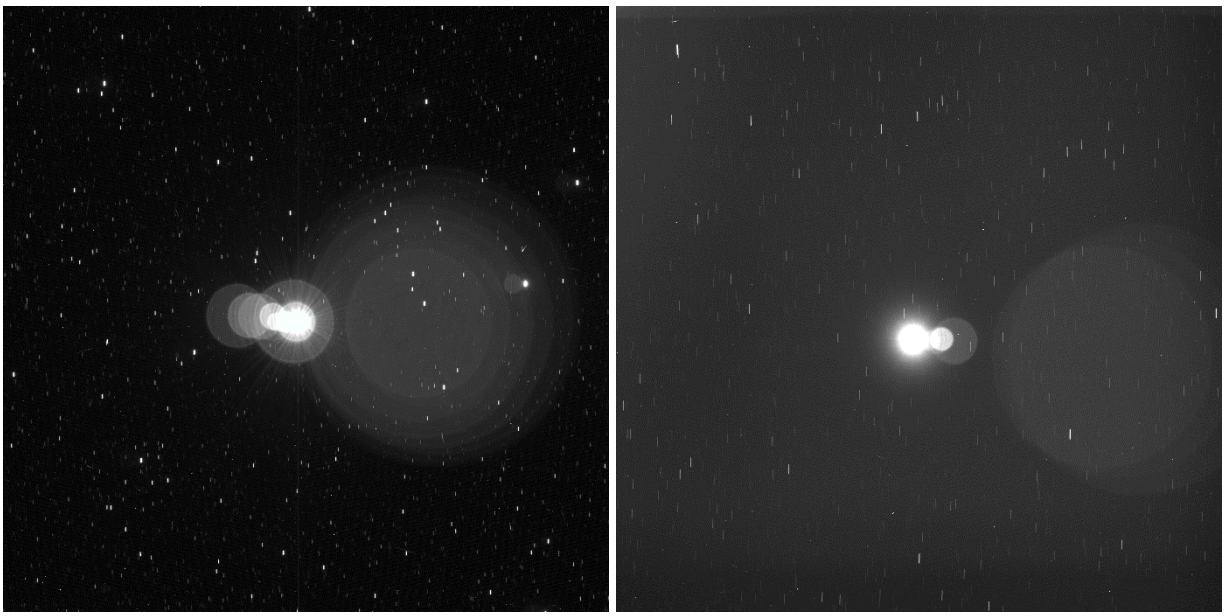

Figure 4 In-field stray-light patterns of the NAC (left) and WAC (right). The images are displayed in the Rosetta standard orientation.

The analysis of the OSIRIS images indicates that even though ghosts and narcissus effects (e.g. reflections from the detector) are small, the additional parasitic flux needs to be corrected for in particular for limb observations and the faint shadows on the nucleus surface. The in-field stray light is as well significant in case of gas and dust observations, where the comet nucleus is strongly overexposed. The contribution of each individual pixel to the ghost is small. However, the integrated values for an extended object can reach up to several percent of the original signal. In shadowed or non-illuminated areas, where the original signal is low, the ghost contribution, from the illuminated surface in the vicinity, can be as high as the original signal.

Lutetia images were used to estimate the in-field stray-light contribution near the limb. The flux close to the limb was measured and compared to the flux of the illuminate surface. The analysis revealed that the effect is wavelength (filter) dependent: the in-field stray light is the lowest in the visible bands, and higher in the UV and NIR bands. Evenly illuminated (flat) artificial images were created and used to estimate the in-field stray-light contribution using the same algorithm that is applied to science data. The integrated ghost pattern intensities (Table 1) are in agreement with the stray light estimated using Lutetia images.

Table 1 Estimate stray light for evenly illuminated image

Camera	Filter	Additional Signal
NAC	F23 (Green)	0.009
NAC	F41 (Near_IR – FFP_IR)	0.031
NAC	F16 (FFP_UV – NearUV)	0.046
WAC	F21 (Green)	0.0039
WAC	F12 (Red)	0.0081
WAC	F71 (UV325)	0.023

3 In-field stray-light removal method

For the in-field stray-light removal, a convolution-based ghost estimation and removal algorithm, similar to the one used for the Dawn Framing Cameras [RD4] has been developed. The method assumes that the detected image (I_{det}) can be expressed as the sum of a series of images, where the first term (I_0) is the expected ghost-free image, followed by the first order ghost (I_{R1}) and the multiple reflection images (I_{Rn}):

$$I_{det} = I_0 + I_{R1}(I_0) + I_{Rn}(I_{Rn-1}) \qquad \text{with } n \geq 2$$

Since the ghost effect is much smaller than the ghost-free image, the second and higher order reflected images are negligible compared to the first two terms. The ghost-free image can be calculated by subtracting the first order ghost contribution from the detected image. The ghost effect computation method is based on the fact that each small detector area, illuminated by a point source, produces similar reflected light intensity distribution and this light intensity distribution is a linear function of the illumination flux of the source. This means that the CCD and filter surfaces behave like a uniform mirror. In this case, the first order ghost image is formed as the convolution of the ghost-free image and the point source stray-light function, i.e. the stray-light image generated by a point source.

$$I_{R1}(x,\mathrm{y}) = \iint I_0(x-x', y-y')P_s(x', y')dx'dy'$$

Each illuminated pixel generates similar reflected intensity distribution (P_s point source stray-light function) scaled by the pixel flux. These partial reflection images add up and form the first reflection image*:* $I_{R1}(I_0)$.
Since the stray energy content is relatively low compared to the ghost-free image, as a first approximation, we can use the detected image as the first estimate of the ghost-free image in the convolution.

$$I_0 \approx I_{det} - I_{det} * P_s$$

The accuracy can be further improved by a second iteration, using the I_0 result of the first calculation. Key to the effective stray-light removal is the accurate determination of the P_s point source stray-light function, or the ghost convolution kernel.

4 In-field stray-light analysis and the ghost kernels

In-flight science and calibration data and on-ground calibration images acquired using the OSIRIS GRM were used to quantitatively characterize the NAC and WAC in-field stray-light patterns. The point source stray-light functions (P_s) for each filter combination were estimated based on those images, and stored in the ghost kernel files.

Calibration campaigns were carried out at MPS in November 2015, using the WAC GRM, and in September 2018, using the NAC GRM. A stray-light experimental setup was built using a fiber optic light source, which served as a point source target in the focus of the OSIRIS mirror collimator. Images were acquired with different exposure times to reveal the different intensity ghost pattern components. The field position dependency of the pattern was also tested and confirmed using a small refractive optical system.

The in-flight calibration images revealed that there are slight alignment differences between the GRM and the FM cameras, which resulted in small shifts in the ghost pattern sizes and positions. In addition, the reflectivity values of the different ghost components are slightly different. Therefore the final ghost pattern geometry and the intensity values were refined using the in-flight calibration images. The ghost kernel files were tested on Lutetia images, which provided background (coma) free, partially filled full frame targets, with high contrast limb. Table 2 and Table 3 contain the list of calibration images that have been used to determine the NAC and WAC ghost kernels.

4.1 Analysis of calibration image

- The calibration images are bias subtracted and normalized to 1 s exposure time.
- The strongest stray-light reflection paths are identified, and matched with the calibration image pattern. Each individual ghost component is represented by a single (circular) feature.
- The sizes (in pixels) of the ghost components are measured in the image.
- The positions of the centres of the ghost components, relative to the point source image, are measured.
- The average intensity of each ghost component is measured and scaled to the point source illumination.
- The size of the full in-field stray-light pattern (containing all the ghost components) is measured relative to the point source image.

The size, position and intensity of each ghost component is stored in vector graphic form in the ghost kernel file (for details see Sec. 6).

4.2 Ghost kernel image determination

The ghost kernel file is used to generate the convolution kernel or ghost kernel image (P_s), which is assembled as a sum of stray-light components. The ghost kernel image is used for the numerical convolution.

For NAC filters F31 and F81, ARP reflection ghosts are taken from the filters closest in wavelength as no calibration data has been acquired. For these filters, reflections from the band-pass filters are not accounted for.

Table 2 GRM calibration images used for ghost kernel calculation

Session	Camera	First image	Last image	# images
session_GRM_20180821_ calibration_prep	NAC	NAC_2018-08-29T09.48.22.985Z_ ID00_1398669000_F23.img	NAC_2018-08-30T15.22.36.062Z_ ID00_1398669002_F84.img	277
session_GRM_20180910_ calib_ghost	NAC	NAC_2018-09-12T09.04.39.787Z_ ID00_1398669000_F21.img	NAC_2018-09-12T12.15.02.427Z_ ID00_1398669004_F84.img	125
session_20151119_GRM__ OC_PointSourceTest	WAC	WAC_2015-11-23T09.37.46.822Z_ ID00_1398669000_F12.img	WAC_2015-11-23T15.26.50.041Z_ ID00_1398669000_F81.img	115

Table 3 In-flight calibration images used for ghost kernel calculation

Observation	Camera	First image	Last image	# images
STEINS_AST1_2008_09	NAC	NAC_2008-09-05T16.55.03.453Z_ ID10_0166015000_F21.IMG	NAC_2008-09-05T16.58.18.203Z_ ID10_0166015003_F21.IMG	4
STEINS_AST1_2008_09	WAC	WAC_2008-09-05T18.16.06.977Z_ ID10_0166045000_F12.IMG	WAC_2008-09-05T18.17.19.338Z_ ID10_0166045003_F12.IMG	4
LUTETIA_AST2_2010_07	WAC	WAC_2010-07-10T11.29.41.261Z_ ID10_1251276000_F12.IMG	WAC_2010-07-10T11.29.56.543Z_ ID10_1251276002_F12.IMG	3
LUTETIA_AST2_2010_07	NAC	NAC_2010-07-10T15.22.40.560Z_ ID10_1251276000_F82.IMG	NAC_2010-07-10T15.45.09.210Z_ ID10_1251276000_F22.IMG	76
STP003_CALIB_GHOST	NAC	NAC_2014-05-14T02.00.57.546Z_ ID10_1397549000_F22.IMG	NAC_2014-05-14T02.05.32.747Z_ ID10_1397549000_F23.IMG	16
STP003_CALIB_GHOST	WAC	WAC_2014-05-14T02.22.02.856Z_ ID10_1397549000_F12.IMG	WAC_2014-05-14T03.32.03.372Z_ ID10_1397549000_F13.IMG	16
STP056_GHOST_911cC	WAC	WAC_2015-05-19T14.48.08.433Z_ ID10_1397549000_F17.img	WAC_2015-05-19T15.37.32.343Z_ ID10_1397549005_F15.img	6
STP056_GHOST_911cTR	WAC	WAC_2015-05-19T15.53.06.661Z_ ID10_1397549000_F13.img	WAC_2015-05-19T16.13.00.545Z_ ID10_1397549002_F13.img	3
STP088_EARTH_001	NAC	NAC_2015-12-29T20.02.08.560Z_ ID10_1397549000_F22.IMG	NAC_2015-12-29T20.06.46.878Z_ ID10_1397549006_F24.IMG	21
STP092_EARTH_001	NAC	NAC_2016-01-23T06.43.42.552Z_ ID10_1397549000_F82.IMG	NAC_2016-01-23T06.49.15.479Z_ ID10_1397549031_F88.IMG	32

5 In-field stray-light removal implementation

The stray-light computation is implemented as a two dimensional numerical convolution of the original image and the convolution kernel (ghost kernel image). The result of the convolution is the ghost image, which contains only the ghost contribution, and that is subsequently subtracted from the original image. This algorithm is computation intensive, and takes significantly more time than the regular calibration steps. Therefore, the generation of the ghost images is handled separately from the calibration pipeline.

A stand-alone application (GhostCrawler) has been developed to generate ghost images for all NAC and WAC images under the following conditions:

- Image is full frame
- Image does not contain missing segments
- Image is not acquired for calibration purposes, identified by TARGET_TYPE = CALIBRATION in the image header
- Ghost kernel exists for filter combination (see Sect. 7)

These ghost images are stored off-line and used by OsiCalliope for the in-field stray-light removal calibration step. Ghost images have the same filename of the original image, but "ID" is replaced with "GS". The number of iteration is recorded in the image header history section:

NUMBER_ITERATIONS = "2"

In addition, for images of 67P GhostCrawler generates synthetic images of the comet nucleus, using SPICE, the 67P shape model and a 67P surface reflectivity model. These are created under the following conditions:

- Any of the conditions listed for ghost images above
- The TARGET_NAME is "67P/CHURYUMOV-GERASIMENKO 1 (1969 R1)"
- The image is from the comet phase (START_TIME > 2014-03-19)
- Shutter operation mode is neither UNK (any camera) nor Type C (NAC only)

If the nucleus is not in the field of view, the synthetic image is equal to zero. The pixel data is stored as 32 bit PC_REAL. The filename of the synthetic image is the same as the original image, but "ID" is replaced with "SY".

The ghost image calculation is done in the following steps:

1. GhostCrawler generates a partially calibrated image from the OSIRIS Level 1 (CODMAC L2) binary by applying the bias, ADC, flat field, bad pixel, and exposure time correction. These are the same calibration steps that are applied by OsiCalliope to calibrate the images. GhostCrawler and OsiCalliope share the same calibration database, to assure consistency. In case the image cannot be exposure time calibrated, no ghost image is generated.
2. GhostCrawler implements a "brute force" multithreaded numerical convolution of the compressed (binned) image and the ghost image (P_s convolution kernel) to calculate the first estimate of the ghost contribution (I_{R1}). The binning used in this step is recorded in the header keyword

   GHOST_BINNING = "2x2"

   (Example)

3. GhostCrawler subtracts the un-binned ghost contribution from the image, and repeats the convolution without the binning.
4. The resulting ghost image is stored for later processing by OsiCalliope.

The ghost image can be generated using either the original image or the synthetic image in the convolution. When the original image is used and it contains saturated pixels, the intensity of the ghost pattern is underestimated.

For images of 67P taken in comet phase, in which the nucleus is in the field of view, if the number of saturated pixels is above 1%, GhostCrawler uses the previously generated synthetic image in the convolution to generate the ghost image.

This is frequently the case for gas and dust observations, where long exposure times were used to reveal the low intensity structures around the comet.

If the synthetic image is used, it is recorded in the keyword

SYNTHETIC_IMAGE = 'NAC_2014-07-29T10.01.46.327Z_SY10_1397549200_F22.IMG'

(Example)

If either the nucleus is not in the field of view or the image target is not 67P (and therefore no synthetic image is available) GhostCrawler uses the original image for the determination of the ghost image. However, in the case in which saturated pixels are present the intensity of the ghost pattern is underestimated.

6 Ghost kernel files description

GhostCrawler uses the ghost kernel files to generate the ghost kernel raster image (convolution kernel) for the removal algorithm.

The ghost kernels are stored in text files containing vector graphics description of the significant ghost pattern components (7 components for WAC and 8 for NAC). The data lines (**GHOSTSPOTnnnn**) are describing the ghost reflection components of a single pixel, reduced to 1 DN flux. The ghost kernel image is generated as a float image with the size of (**IMAGESIZE_X, IMAGESIZE_Y**), which is the minimum size encapsulating all the pattern components. The size is different for NAC and WAC. The numerical convolution is carried out on the original full frame, un-binned image, and the kernel image, with the kernel center at **VECTOR_OFFSET**. The kernel center is the center coordinate of the 2D convolution for the kernel image. During the rasterization the ghost component intensities are calculated as the product of a general scaling parameter (**INTENSITY_SCALE**) and the relative intensity of the ghost spot (**P11**). After generating the ghost kernel image with the ghost components, a Gaussian blur is applied to smooth the pattern edges. The radius of the blur filter is **BLUR_EDGES**.

The ghost kernel image size in pixels:

IMAGESIZE_X = 1300

IMAGESIZE_Y = 1000

Kernel center in pixels:

VECTOR_OFFSET = (350, 500)

Radius of the blur filter in pixels:

BLUR_EDGES = 5

Pixel stretching center:

VECTOR_STRETCH = (0, 0)

General intensity scale for the full kernel:

INTENSITY_SCALE = 2.3e-9

Number of **GHOSTSPOTnnnn** components:

VECTOR_COUNT = 17

The individual vector components (n = 0 - **VECTOR_COUNT** -1):

GHOSTSPOT000n = ("VectorType", P0, P1, P2, P3, P4, P5, P6, P7, P8, P9, P10, P11, P12)

Where:

VectorType: Marker, CircleDraw, CircleFill, EllipseDraw, EllipseFill

P0, P1, P2, P3, P4, P5: vector geometry (x,y coordinates, sizes, radius, rotation)

P6, P7, P8, P9: additional position stretching parameters

P10 : display color RGB DWORD (used only for display)

P11 : pattern component relative intensity

P12 : display flag (0: used for calculation; 1: display only)

7 Calibration files used by OsiCalliope and GhostCrawler

The data (ghost kernel) files used for the in-field stray-light removal of OSIRIS images are:

- NAC_FM_GHOST_15_V01.TXT
- NAC_FM_GHOST_16_V01.TXT
- NAC_FM_GHOST_22_V01.TXT
- NAC_FM_GHOST_23_V01.TXT
- NAC_FM_GHOST_24_V01.TXT
- NAC_FM_GHOST_27_V01.TXT
- NAC_FM_GHOST_28_V01.TXT
- NAC_FM_GHOST_31_V01.TXT
- NAC_FM_GHOST_32_V01.TXT
- NAC_FM_GHOST_33_V01.TXT
- NAC_FM_GHOST_34_V01.TXT
- NAC_FM_GHOST_37_V01.TXT
- NAC_FM_GHOST_38_V01.TXT
- NAC_FM_GHOST_41_V01.TXT
- NAC_FM_GHOST_51_V01.TXT
- NAC_FM_GHOST_61_V01.TXT
- NAC_FM_GHOST_71_V01.TXT
- NAC_FM_GHOST_81_V01.TXT
- NAC_FM_GHOST_82_V01.TXT
- NAC_FM_GHOST_83_V01.TXT
- NAC_FM_GHOST_84_V01.TXT
- NAC_FM_GHOST_87_V01.TXT
- NAC_FM_GHOST_88_V01.TXT

- WAC_FM_GHOST_11_V01.TXT
- WAC_FM_GHOST_12_V01.TXT
- WAC_FM_GHOST_13_V02.TXT
- WAC_FM_GHOST_14_V02.TXT
- WAC_FM_GHOST_15_V01.TXT
- WAC_FM_GHOST_16_V01.TXT
- WAC_FM_GHOST_17_V01.TXT
- WAC_FM_GHOST_18_V01.TXT
- WAC_FM_GHOST_21_V01.TXT
- WAC_FM_GHOST_31_V01.TXT
- WAC_FM_GHOST_41_V01.TXT
- WAC_FM_GHOST_51_V01.TXT
- WAC_FM_GHOST_61_V01.TXT
- WAC_FM_GHOST_71_V01.TXT
- WAC_FM_GHOST_81_V01.TXT

The files are included in each public delivery of OSIRIS data to PSA. The location is specified in the OSIRIS EAICD [RD3].